

Elvira Barbera · Francesca Brini

## On stationary heat conduction in 3D symmetric domains: an application of extended thermodynamics

Received: 15 July 2009 / Revised: 29 March 2010 / Published online: 4 June 2010  
© Springer-Verlag 2010

**Abstract** In this paper, we study some three-dimensional stationary heat conduction problems in rarefied gases at rest, using the linearized 13-moment equations of extended thermodynamics. It follows that, in this linear theory, the temperature is still described by the Fourier law of heat conduction, while in contrast with the Navier–Stokes law, the stress tensor does not vanish. Furthermore, a non-equilibrium temperature is introduced and differences between this temperature and the kinetic one are predicted.

### 1 Introduction

The heat conduction problem represents an interesting and important topic of thermodynamics, both from a theoretical and an experimental point of view. Historically, one referred to the classical thermodynamics in order to describe such a phenomenon mathematically. Following this classical theory, the field equations are based on the conservation laws of mass, momentum and energy, while the closure of the system is obtained thanks to the Navier–Stokes and the Fourier laws. However, it was observed that while the Navier–Stokes–Fourier (NSF) approximations are in complete agreement with the experimental results for dense gases, they are not appropriate for rarefied cases or when strong deviations from equilibrium occur.

In the last 70 years, different non-equilibrium theories have been proposed in order to have a more suitable description of thermodynamic phenomena that involve rarefied gases or processes far from equilibrium. In our knowledge, the first non-equilibrium thermodynamic theory goes back to the 1940s, when Eckart [1] incorporated the Navier–Stokes–Fourier laws in a consistent thermodynamic scheme. This theory is known as thermodynamics of irreversible processes (TIP). It used the Gibbs equations together with the principle of local equilibrium and combines them with the balance equations of mass, momentum and energy deriving the Clausius–Duhem inequality. Then TIP ensures the non-negative entropy production assuming only linear relations between forces and fluxes. In this way, one obtains constitutive relations that coincide with the Navier–Stokes and Fourier equations. A detailed explanation of this theory can be found, for example, in a recent book about the history of thermodynamics [2] and in [3].

Straight afterward two different non-equilibrium thermodynamic approaches were proposed, they are due to Meixner [4] and to Prigogine [5]. These theories can also be found in the book of de Groot and Mazur [6].

---

E. Barbera (✉)  
Di.S.I.A., Università degli Studi di Messina,  
c/dia di Dio, S. Agata, 98166 Messina, Italy  
E-mail: ebarbera@unime.it

F. Brini  
Dipartimento di Matematica and C.I.R.A.M.,  
Università degli Studi di Bologna,  
via Saragozza 8, 40123 Bologna, Italy  
E-mail: brini@ciram.unibo.it

Some years later, in the 1960s, another non-equilibrium theory, called rational thermodynamics (RT), was formulated [7,8]. The main difference between this theory and TIP is that RT postulates the validity of an entropy inequality, the Clausius–Duhem inequality and derives from it the Gibbs equation.

In 1966 Müller [9] tried to derive modifications of the Navier–Stokes and Fourier equations from the principle of TIP. He noticed that without the principle of local equilibrium, TIP can be used to derive Cattaneo-like equations. This theory is known as Extended TIP. A detailed explanation of it, together with some criticisms, can be found in [3].

In this paper, we will refer to rational extended thermodynamics [3] (RET). RET considers as field variables not only the classical ones (mass densities, momentum and energy) but also the stress tensor, the heat flux and others. The corresponding field equations are balance laws supplemented by local and instantaneous constitutive equations. Such constitutive functions are determined through the validity requirement of universal physical principles, such as the entropy principle (existence of an entropy inequality and concavity of the entropy density) and the principle of relativity. In the study [3], the connection of this theory with RT is discussed. In particular, although the two theories are different, they both postulate the validity of the entropy inequality and recover from it the constitutive relations. In RET the exploitation of the entropy principle is made by use of the Lagrange multipliers [10] (also called main fields). Referring to these privileged main field components, it is possible to rewrite the field equations in the form of a symmetric hyperbolic system [11,12]. Hyperbolicity guarantees finite speeds of propagation and symmetric hyperbolic systems have convenient and desirable mathematical properties, namely well-posedness of Cauchy problems, i.e. existence, uniqueness, and continuous dependence on the data. A well-known application of Rational Extended Thermodynamics is Extended Thermodynamics of Moments, where the field variables are the moments of a distribution function. In the study [3], the authors presented a full exploitation of this case with an arbitrary number of moments. In the particular case of 13 moments, that will be considered in this paper, RET coincides with the well-known theory of Grad [13,14]. This fact is shown with details at the beginning of the next section.

We have to stress that other different non-equilibrium thermodynamics approaches that extend the number of field variables were proposed in the literature. Among the others, we recall extended irreversible thermodynamics [15–18] and thermodynamics with the internal variables [19–22].

In particular, in extended irreversible thermodynamics [15–18], the heat flux and the stress tensor are used as field variables too, but the equations for them are recovered through a procedure similar to TIP. A generalized entropy is introduced, and the generalized Gibbs equation is postulated. The new field equations are obtained from the generalized Clausius–Duhem inequality assuming linear relations between forces and fluxes.

Rational extended thermodynamics has been tested in many physical fields and it turns out to be more suitable than classical thermodynamics for the description of rarefied gases [3]; we recall, for example, light scattering [23,24], shock waves and shock structures [25], phonon theory [26,27]. Moreover RET has been applied also to relativistic phenomena [28], chemically reacting mixtures of gases [29], radiation phenomena [30,31], plane Couette flow [32] and convection phenomena [33].

In the last 10 years, after a paper by Donato and Ruggeri [34], it has been noticed that even the simplest model of rational extended thermodynamics (the 13-moment theory) predicts different results from classical thermodynamics. A comparison between 13-moment and Navier–Stokes–Fourier theories was made in the simplest non-equilibrium thermodynamic problem: that is to say in the stationary heat conduction problem of a monatomic classical ideal gas. The differences between the theories become evident when the phenomenon takes place in some special curved domains [35–37]. In particular, Müller and Ruggeri [35] studied the stationary heat conduction problem for a rarefied gas at rest in the gap between two coaxial circular cylinders or two concentric spheres. In this special case, the equations reduce to an ODE system and the solution can be determined analytically. It was found that the normal components of the stress tensor, which are zero in the classical theory, do not vanish in the 13-moment case and consequently the Fourier law is no more valid. Barbera and Müller [36] analyzed the stationary heat conduction between two coaxial rotating cylinders. They showed that no rigid rotation of the heat conducting gas is compatible with the Grad's equations, in contrast with NSF. Finally, Barbera and Müller [37] showed that, also in the neighborhood of equilibrium, classical and extended thermodynamics differ in the case of stationary heat conduction between two confocal elliptical cylinders. The aim of the present paper is to generalize these previous works [35,37], in order to understand if these effects are a peculiarity of certain special geometries or they are present in all the curved domains. We will focus our attention on the stationary heat conduction problem for a gas at rest in three-dimensional domains provided with geometric symmetries: non-coaxial circular cylinders, confocal ellipsoids and non-concentric spheres. In these cases, the complete 13-moment equations present fine mathematical problems for phenomena far from an equilibrium state. Nevertheless, as already said, we are interested on the comparison between classical and

extended thermodynamics. Therefore, we will consider the linearized field equations in the neighborhood of equilibrium, since already in this case significant differences are observed. Moreover, in the linear case, it is possible to determine the solutions analytically, at least for the domains and for the boundary conditions we have chosen.

Because of the linear approximation, the temperature behavior of the 13-moment equations coincides with that of the Fourier theory. Nonetheless, the normal and shear components of the deviatoric stress tensor do not vanish, unlike the classical case. Besides, we found a difference between the kinetic temperature—a measure for the mean kinetic energy of the atoms—and the non-equilibrium temperature.

## 2 Grad's 13-moment field equations

The fields of extended thermodynamics for monatomic ideal gases [3] are moments of the distribution function  $f(\mathbf{x}, \mathbf{C}, t)$  of the gas, defined as

$$\rho_{i_1 i_2 \dots i_N} = m \int C_{i_1} C_{i_2} \dots C_{i_N} f d\mathbf{C}, \quad (1)$$

where  $m$  is the atomic mass of the gas,  $\mathbf{C}$  is the velocity of the atoms relative to the gas velocity and  $f(\mathbf{x}, \mathbf{C}, t)d\mathbf{C}$  represents the number density of the atoms at  $\mathbf{x}$  and  $t$  with velocity  $\mathbf{C}$ .

Some of these moments can be easily related to more common thermodynamic fields. Thus,  $\rho$  is the mass density,  $\rho_{ij}$  is the pressure tensor with its trace  $\rho_{ll} = 3p$ , where  $p$  is the pressure, and with the traceless part<sup>1</sup>  $\rho_{\langle ij \rangle}$  equal to the stress tensor,  $\rho_{ill} = 2q_i$ ,  $q_i$  being the heat flux. Furthermore,  $\rho_i = 0$  since  $\mathbf{C}$  is the relative velocity.

The field equations of extended thermodynamics are derived from the Boltzmann equation that for a gas at rest assumes the form

$$\frac{\partial f}{\partial t} + c_k \frac{\partial f}{\partial x_k} = -\frac{f - f^E}{\tau} \quad \text{with} \quad f^E = \frac{\rho}{m} \frac{1}{\sqrt{2\pi \frac{k_B}{m} T}} e^{-\frac{C^2}{2\frac{k_B}{m} T}}, \quad (2)$$

where  $c_k$  is the velocity of the atoms. Here  $c_k = C_k$  since the gas is at rest. The right hand side of (2) represents the production term due to collisions. Since in our problem the nature of the interactions between the molecules is quite irrelevant, we have chosen the simplest one based on the BGK approximation [38]. It assumes that the net effect of collisions is to make the distribution function  $f$  relax toward the equilibrium distribution function  $f^E$  with a constant characteristic time  $\tau$  equal to the mean time of free flight. In (2)  $2k_B$  is the Boltzmann constant and  $T$  is usually called the kinetic temperature, since  $3/2 k_B T$  is the mean kinetic energy of the atoms. In the following, for simplicity, we will use  $\theta = \frac{k_B}{m} T$  instead of  $T$ .

By multiplication of (2) with  $C_{i_1} C_{i_2} \dots C_{i_N}$  and integration over the whole range of the velocity, one derives the complete hierarchy of balance equations for the moments that for a gas at rest assumes the form

$$\frac{\partial \rho_{i_1 i_2 \dots i_N}}{\partial t} + \frac{\partial \rho_{i_1 i_2 \dots i_N k}}{\partial x_k} = -\frac{\rho_{i_1 i_2 \dots i_N} - \rho_{i_1 i_2 \dots i_N}^E}{\tau}. \quad (3)$$

The symbol 'E' represents equilibrium and  $\rho_{i_1 i_2 \dots i_N}^E$  are the moments (1) evaluated for  $f = f^E$ .

In this paper, we limit our analysis to extended thermodynamics with 13 moments, i.e. we consider as field variables the first 13 moments of (1):  $\rho$ ,  $\rho_i = 0$ ,  $p$ ,  $\rho_{\langle ij \rangle}$  and  $q_i$ . Thus, the field equations are the first 13 of (3), and for a stationary problem in a gas at rest they read

$$\frac{\partial \rho_i}{\partial x_k} = 0, \quad \frac{\partial p}{\partial x_i} + \frac{\partial \rho_{\langle ik \rangle}}{\partial x_k} = 0, \quad \frac{\partial q_k}{\partial x_k} = 0, \quad \frac{\partial \rho_{\langle ij \rangle k}}{\partial x_k} = -\frac{\rho_{\langle ij \rangle}}{\tau}, \quad \frac{\partial \rho_{ikl}}{\partial x_k} = -2\frac{q_i}{\tau}. \quad (4)$$

The first equation represents the conservation law of mass and it is identically satisfied since  $\rho_i = 0$ , thus, in the following we will not consider this equation anymore. The second is the conservation law of momentum. Equations (4)<sub>3,4</sub> are respectively the trace and the traceless part of (3) for  $N = 2$ . The trace represents the

<sup>1</sup> The angular brackets stand for the traceless part of a symmetric tensor.

conservation law of energy, while (4)<sub>4</sub> is the balance law for the stress tensor. Finally, equation (4)<sub>4</sub> is the balance law for the heat flux.

This system is not closed due to the presence of the moments  $\rho_{\langle ij \rangle k}$  and  $\rho_{ikll}$ . It can be closed determining such moments from the Grad 13-moments distribution function [13,14] that reads

$$f^G = f^E \left[ 1 + \frac{1}{2p\theta} \rho_{\langle ij \rangle} C_i C_j - \frac{1}{p\theta^2} q_i C_i \left( 1 - \frac{C^2}{5\theta} \right) \right]. \quad (5)$$

Substituting this distribution function in the definition of the moments (3) one obtains the constitutive functions

$$\rho_{\langle ij \rangle k} = \frac{2}{5} \left( q_i \delta_{jk} + q_j \delta_{ik} - \frac{2}{3} q_k \delta_{ij} \right), \quad \rho_{ikll} = 5p\theta \delta_{ik} + 7\theta \rho_{\langle ik \rangle}, \quad (6)$$

where  $\delta_{ik}$  denotes the Kronecker tensor.

System (4, 6) represents a closed system of field equations for the fields  $p, \theta, \rho_{\langle ij \rangle}$  and  $q_i$ . For simplicity, we have considered  $\theta$  instead of  $\rho$  as field variable and this can be done in a ideal gas where  $\rho = p/\theta$ .

For further purpose, we rewrite the field equations (4, 6) in the curvilinear coordinates  $z^k$ , so that they assume the form

$$\begin{aligned} g^{ik} \frac{\partial p}{\partial z^k} + \rho_{;k}^{\langle ik \rangle} &= 0, \\ q_{;k}^k &= 0, \\ \rho_{;k}^{\langle ij \rangle k} &= -\frac{1}{\tau} \rho^{\langle ij \rangle}, \quad \text{with} \quad \rho^{\langle ij \rangle k} = \frac{2}{5} \left( q^i g^{jk} + q^j g^{ki} - \frac{2}{3} q^k g^{ij} \right), \\ \rho_n^{ikn} &= -\frac{2}{\tau} q^k, \quad \text{with} \quad \rho_n^{ikn} = 5p\theta g^{ik} + 7\theta \rho^{\langle ik \rangle}. \end{aligned} \quad (7)$$

Here upper and lower indices represent contra- and co-varient components of the tensors,  $g^{ik}$  is the metric tensor (as usual,  $g^{ik} g_{kj} = \delta_j^i$ , with  $\delta_j^i$  the Kronecker symbol) and the semicolon denotes covariant derivative with respect to  $z^k$ .

We will consider the heat conduction problem in different domains that share the common property to be described by suitable orthogonal coordinates satisfying the following properties:

$$g^{11} = g^{22}, \quad \frac{\partial g^{11}}{\partial z^3} = \frac{\partial g^{22}}{\partial z^3} = \frac{\partial g^{33}}{\partial z^3} = 0. \quad (8)$$

Thus, the non-vanishing Christoffel symbols can be expressed in terms of only four of them by the relations

$$\begin{aligned} \Gamma_{11}^1 &= -\Gamma_{22}^1 = \Gamma_{12}^2 = \Gamma_{21}^2, & \Gamma_{22}^2 &= -\Gamma_{11}^2 = \Gamma_{12}^1 = \Gamma_{21}^1, \\ \Gamma_{33}^1 &= -\frac{g^{11}}{g^{33}} \Gamma_{13}^3 = -\frac{g^{11}}{g^{33}} \Gamma_{31}^3, & \Gamma_{33}^2 &= -\frac{g^{22}}{g^{33}} \Gamma_{23}^3 = -\frac{g^{22}}{g^{33}} \Gamma_{32}^3. \end{aligned} \quad (9)$$

In all these cases, we will suppose that the boundary manifolds of the domains are kept at a constant temperature (as frequently done in the experiments). So, thanks to this assumption and to the geometric symmetry of the regions, the study of the heat conduction in three-dimensional space reduces to a bi-dimensional problem requiring that

$$q^3 = 0, \quad \frac{\partial \cdot}{\partial z^3} = 0. \quad (10)$$

Hence, system (7) can be written explicitly as

$$\begin{aligned}
& g \frac{\partial p}{\partial z^1} + \frac{\partial \rho^{(11)}}{\partial z^1} + \frac{\partial \rho^{(12)}}{\partial z^2} + (3\Gamma_{11}^1 + 2\Gamma_{31}^3) \rho^{(11)} + (4\Gamma_{22}^2 + \Gamma_{32}^3) \rho^{(12)} + (\Gamma_{31}^3 - \Gamma_{11}^1) \rho^{(22)} = 0, \\
& g \frac{\partial p}{\partial z^2} + \frac{\partial \rho^{(12)}}{\partial z^1} + \frac{\partial \rho^{(22)}}{\partial z^2} + (4\Gamma_{11}^1 + \Gamma_{31}^3) \rho^{(12)} + (3\Gamma_{22}^2 + 2\Gamma_{32}^3) \rho^{(22)} + (\Gamma_{32}^3 - \Gamma_{22}^2) \rho^{(11)} = 0, \\
& \frac{\partial q^1}{\partial z^1} + \frac{\partial q^2}{\partial z^2} + (2\Gamma_{11}^1 + \Gamma_{31}^3) q^1 + (2\Gamma_{22}^2 + \Gamma_{32}^3) q^2 = 0, \\
& \frac{4}{5} g \left( \frac{\partial q^1}{\partial z^1} + \Gamma_{11}^1 q^1 + \Gamma_{22}^2 q^2 \right) = -\frac{1}{\tau} \rho^{(11)}, \\
& \frac{2}{5} g \left( \frac{\partial q^2}{\partial z^1} + \frac{\partial q^1}{\partial z^2} \right) = -\frac{1}{\tau} \rho^{(12)}, \\
& \frac{4}{5} g \left( \frac{\partial q^2}{\partial z^2} + \Gamma_{11}^1 q^1 + \Gamma_{22}^2 q^2 \right) = -\frac{1}{\tau} \rho^{(22)}, \\
& 5gp \frac{\partial \theta}{\partial z^1} - 2g\theta \frac{\partial p}{\partial z^1} + 7\rho^{(11)} \frac{\partial \theta}{\partial z^1} + 7\rho^{(12)} \frac{\partial \theta}{\partial z^2} = -\frac{2}{\tau} q^1, \\
& 5gp \frac{\partial \theta}{\partial z^2} - 2g\theta \frac{\partial p}{\partial z^2} + 7\rho^{(12)} \frac{\partial \theta}{\partial z^1} + 7\rho^{(22)} \frac{\partial \theta}{\partial z^2} = -\frac{2}{\tau} q^2,
\end{aligned} \tag{11}$$

with  $g = g^{11} = g^{22}$ .

It is well known that in some cases the contravariant and the covariant components of vectors and tensors do not have an immediate physical meaning and usually their physical dimensions do not coincide with those of the vector or of the tensor to which they refer. For this reason, we will rewrite equations (11) in terms of physical components [39,40] defined as

$$\hat{q}^i = \sqrt{g_{ii}} q^i, \quad \hat{\rho}^{ik} = \sqrt{g_{ii}} \sqrt{g_{kk}} \rho^{ik}, \tag{12}$$

where the underlined indices are unsummed. Then, system (11) becomes

$$\begin{aligned}
& \frac{\partial p}{\partial z^1} + \frac{\partial \hat{\rho}^{(11)}}{\partial z^1} + \frac{\partial \hat{\rho}^{(12)}}{\partial z^2} + (\Gamma_{11}^1 + 2\Gamma_{31}^3) \hat{\rho}^{(11)} + (2\Gamma_{22}^2 + \Gamma_{32}^3) \hat{\rho}^{(12)} + (\Gamma_{31}^3 - \Gamma_{11}^1) \hat{\rho}^{(22)} = 0, \\
& \frac{\partial p}{\partial z^2} + \frac{\partial \hat{\rho}^{(12)}}{\partial z^1} + \frac{\partial \hat{\rho}^{(22)}}{\partial z^2} + (2\Gamma_{11}^1 + \Gamma_{31}^3) \hat{\rho}^{(12)} + (\Gamma_{22}^2 + 2\Gamma_{32}^3) \hat{\rho}^{(22)} + (\Gamma_{32}^3 - \Gamma_{22}^2) \hat{\rho}^{(11)} = 0, \\
& \frac{\partial \hat{q}^1}{\partial z^1} + \frac{\partial \hat{q}^2}{\partial z^2} + (\Gamma_{11}^1 + \Gamma_{31}^3) \hat{q}^1 + (\Gamma_{22}^2 + \Gamma_{32}^3) \hat{q}^2 = 0, \\
& \frac{4}{5} \left( \frac{\partial \hat{q}^1}{\partial z^1} + \Gamma_{22}^2 \hat{q}^2 \right) = -\frac{1}{\tau} \frac{\hat{\rho}^{(11)}}{\sqrt{g}}, \\
& \frac{2}{5} \left( \frac{\partial \hat{q}^2}{\partial z^1} + \frac{\partial \hat{q}^1}{\partial z^2} - \Gamma_{11}^1 \hat{q}^2 - \Gamma_{22}^2 \hat{q}^1 \right) = -\frac{1}{\tau} \frac{\hat{\rho}^{(12)}}{\sqrt{g}}, \\
& \frac{4}{5} \left( \frac{\partial \hat{q}^2}{\partial z^2} + \Gamma_{11}^1 \hat{q}^1 \right) = -\frac{1}{\tau} \frac{\hat{\rho}^{(22)}}{\sqrt{g}}, \\
& 5p \frac{\partial \theta}{\partial z^1} - 2\theta \frac{\partial p}{\partial z^1} + 7\hat{\rho}^{(11)} \frac{\partial \theta}{\partial z^1} + 7\hat{\rho}^{(12)} \frac{\partial \theta}{\partial z^2} = -\frac{2}{\tau} \frac{\hat{q}^1}{\sqrt{g}}, \\
& 5p \frac{\partial \theta}{\partial z^2} - 2\theta \frac{\partial p}{\partial z^2} + 7\hat{\rho}^{(12)} \frac{\partial \theta}{\partial z^1} + 7\hat{\rho}^{(22)} \frac{\partial \theta}{\partial z^2} = -\frac{2}{\tau} \frac{\hat{q}^2}{\sqrt{g}}.
\end{aligned} \tag{13}$$

Let us now introduce the following dimensionless fields and parameters in order to simplify the heat conduction problem:

$$\begin{aligned}\tilde{p} &= \frac{p}{p_0}, \quad \tilde{\rho}^{(ij)} = \frac{\hat{\rho}^{(ij)}}{p_0}, \quad \tilde{q}^i = \frac{\hat{q}^i}{p_0 \sqrt{\frac{k_B}{m} T_0}}, \\ \tilde{T} &= \frac{\theta}{\frac{k_B}{m} T_0}, \quad \tilde{g} = c^2 g, \quad Kn = \tau \frac{\sqrt{\frac{k_B}{m} T_0}}{c},\end{aligned}\tag{14}$$

where  $p_0$ ,  $T_0$  and  $c$  are suitable physical constants that represent respectively a pressure, a kinetic temperature and a length. Such quantities will be defined in detail in the following. We stress that the parameter  $Kn$  in (14) is related to the Knudsen number and it is a good measure for the gas rarefaction. In particular,  $Kn \ll 1$  corresponds to a dense gas, while when the gas is rarefied,  $Kn$  is closer to 1.

In terms of the dimensionless variables (14), system (13) reads

$$\begin{aligned}\frac{\partial \tilde{p}}{\partial z^1} + \frac{\partial \tilde{\rho}^{(11)}}{\partial z^1} + \frac{\partial \tilde{\rho}^{(12)}}{\partial z^2} + (\Gamma_{11}^1 + 2\Gamma_{31}^3) \tilde{\rho}^{(11)} + (2\Gamma_{22}^2 + \Gamma_{32}^3) \tilde{\rho}^{(12)} + (\Gamma_{31}^3 - \Gamma_{11}^1) \tilde{\rho}^{(22)} &= 0, \\ \frac{\partial \tilde{p}}{\partial z^2} + \frac{\partial \tilde{\rho}^{(12)}}{\partial z^1} + \frac{\partial \tilde{\rho}^{(22)}}{\partial z^2} + (2\Gamma_{11}^1 + \Gamma_{31}^3) \tilde{\rho}^{(12)} + (\Gamma_{22}^2 + 2\Gamma_{32}^3) \tilde{\rho}^{(22)} + (\Gamma_{32}^3 - \Gamma_{22}^2) \tilde{\rho}^{(11)} &= 0, \\ \frac{\partial \tilde{q}^1}{\partial z^1} + \frac{\partial \tilde{q}^2}{\partial z^2} + (\Gamma_{11}^1 + \Gamma_{31}^3) \tilde{q}^1 + (\Gamma_{22}^2 + \Gamma_{32}^3) \tilde{q}^2 &= 0, \\ \frac{4}{5} \left( \frac{\partial \tilde{q}^1}{\partial z^1} + \Gamma_{22}^2 \tilde{q}^2 \right) &= -\frac{1}{Kn} \frac{\tilde{\rho}^{(11)}}{\sqrt{\tilde{g}}}, \\ \frac{2}{5} \left( \frac{\partial \tilde{q}^2}{\partial z^1} + \frac{\partial \tilde{q}^1}{\partial z^2} - \Gamma_{11}^1 \tilde{q}^2 - \Gamma_{22}^2 \tilde{q}^1 \right) &= -\frac{1}{Kn} \frac{\tilde{\rho}^{(12)}}{\sqrt{\tilde{g}}}, \\ \frac{4}{5} \left( \frac{\partial \tilde{q}^2}{\partial z^2} + \Gamma_{11}^1 \tilde{q}^1 \right) &= -\frac{1}{Kn} \frac{\tilde{\rho}^{(22)}}{\sqrt{\tilde{g}}}, \\ 5\tilde{p} \frac{\partial \tilde{T}}{\partial z^1} - 2\tilde{T} \frac{\partial \tilde{p}}{\partial z^1} + 7\tilde{\rho}^{(11)} \frac{\partial \tilde{T}}{\partial z^1} + 7\tilde{\rho}^{(12)} \frac{\partial \tilde{T}}{\partial z^2} &= -\frac{2}{Kn} \frac{\tilde{q}^1}{\sqrt{\tilde{g}}}, \\ 5\tilde{p} \frac{\partial \tilde{T}}{\partial z^2} - 2\tilde{T} \frac{\partial \tilde{p}}{\partial z^2} + 7\tilde{\rho}^{(12)} \frac{\partial \tilde{T}}{\partial z^1} + 7\tilde{\rho}^{(22)} \frac{\partial \tilde{T}}{\partial z^2} &= -\frac{2}{Kn} \frac{\tilde{q}^2}{\sqrt{\tilde{g}}}.\end{aligned}\tag{15}$$

For a reader who is not familiar with curvilinear coordinates, we recall that in standard cartesian coordinates all Christoffel symbols vanish. So, in the planar case Eqs. (15) are to be considered with  $\Gamma_{ij}^k = 0$ .

Since the solution of this complete system presents many mathematical problems, in this paper we will study the heat conduction phenomena in the neighborhood of an equilibrium characterized by  $p = p_0$ ,  $\theta = \frac{k_B}{m} T_0$ ,  $\rho^{(ij)} = 0$ ,  $q^i = 0$  and we will linearize system (15). We stress that all the equations in the previous system are linear in the field variables except for the last two. Therefore, equations (15)<sub>1–6</sub> will remain unchanged. On the contrary, the underlined terms in equations (15)<sub>7,8</sub> are negligible in the neighborhood of the equilibrium state, since both the stress deviator components and the temperature derivatives are close to zero. In addition, the remaining terms of (15)<sub>7,8</sub> will be linearized in the neighborhood of  $\tilde{p} = 1$ ,  $\tilde{T} = 1$ , i.e.

$$\begin{aligned}5 \frac{\partial \tilde{T}}{\partial z^1} - 2 \frac{\partial \tilde{p}}{\partial z^1} &= -\frac{2}{Kn} \frac{\tilde{q}^1}{\sqrt{\tilde{g}}}, \\ 5 \frac{\partial \tilde{T}}{\partial z^2} - 2 \frac{\partial \tilde{p}}{\partial z^2} &= -\frac{2}{Kn} \frac{\tilde{q}^2}{\sqrt{\tilde{g}}}.\end{aligned}\tag{16}$$

Inserting (16) into (15)<sub>1–6</sub>, making some lengthy calculations and taking into account that the following relations hold:

$$\begin{aligned} \frac{\partial \Gamma_{11}^1}{\partial z^1} + \frac{\partial \Gamma_{22}^2}{\partial z^2} &= 0, \\ \frac{\partial \Gamma_{31}^3}{\partial z^1} + (\Gamma_{31}^3)^2 - \Gamma_{11}^1 \Gamma_{31}^3 + \Gamma_{22}^2 \Gamma_{32}^3 &= 0, \\ \frac{\partial \Gamma_{31}^3}{\partial z^2} + \Gamma_{31}^3 \Gamma_{32}^3 - \Gamma_{22}^2 \Gamma_{31}^3 - \Gamma_{11}^1 \Gamma_{32}^3 &= 0, \\ \frac{\partial \Gamma_{32}^3}{\partial z^2} + \Gamma_{31}^3 \Gamma_{11}^1 + (\Gamma_{32}^3)^2 - \Gamma_{22}^2 \Gamma_{32}^3 &= 0, \end{aligned} \quad (17)$$

one obtains

$$\begin{aligned} \tilde{p} &= 1, \\ \Delta \tilde{T} = 0 \implies \frac{\partial}{\partial z^1} \left( \frac{1}{\sqrt{g^{33}}} \frac{\partial \tilde{T}}{\partial z^1} \right) + \frac{\partial}{\partial z^2} \left( \frac{1}{\sqrt{g^{33}}} \frac{\partial \tilde{T}}{\partial z^2} \right) &= 0, \\ \tilde{q}^1 &= -\frac{5}{2} Kn \sqrt{\tilde{g}} \frac{\partial \tilde{T}}{\partial z^1}, \\ \tilde{q}^2 &= -\frac{5}{2} Kn \sqrt{\tilde{g}} \frac{\partial \tilde{T}}{\partial z^2}, \\ \tilde{\rho}^{(11)} &= 2Kn^2 \tilde{g} \left[ -\Gamma_{11}^1 \frac{\partial \tilde{T}}{\partial z^1} + \frac{\partial^2 \tilde{T}}{(\partial z^1)^2} + \Gamma_{22}^2 \frac{\partial \tilde{T}}{\partial z^2} \right], \\ \tilde{\rho}^{(12)} &= 2Kn^2 \tilde{g} \left[ -\Gamma_{11}^1 \frac{\partial \tilde{T}}{\partial z^2} + \frac{\partial^2 \tilde{T}}{\partial z^1 \partial z^2} - \Gamma_{22}^2 \frac{\partial \tilde{T}}{\partial z^1} \right], \\ \tilde{\rho}^{(22)} &= 2Kn^2 \tilde{g} \left[ \Gamma_{11}^1 \frac{\partial \tilde{T}}{\partial z^1} + \frac{\partial^2 \tilde{T}}{(\partial z^2)^2} - \Gamma_{22}^2 \frac{\partial \tilde{T}}{\partial z^2} \right]. \end{aligned} \quad (18)$$

The symbol  $\Delta$  represents here the Laplace operator in the  $(z^1, z^2)$ -coordinates.

### 3 Geometrical description, boundary data and heat conduction solutions

In this section, we will refer to the previous Eq. (18) for the study of heat conduction in the gap between two manifolds. In particular, we will focus on different spatial domains that can be described through the introduction of appropriate orthogonal coordinates: confocal elliptical cylinders (the only case for which the linearized theory was already studied [37]), confocal ellipsoids, non-coaxial circular cylinders and non-concentric spheres. In the following subsections these different cases will be analyzed separately introducing the most suitable coordinates, recalling the corresponding Kronecker tensors and Christoffel symbols, determining the analytical solutions and showing the results through bi-dimensional and three-dimensional pictures. For the figures and the comments of Sects. 3.1–3.4 we will always refer to the same parameters values for the Knudsen number, the quantity  $c$  and the two external and internal boundary temperatures that are respectively  $Kn = 0.227$ ,  $c = 0.002$  m,  $\tilde{T}_e = \tilde{T}_0 = 1$  and  $\tilde{T}_i = 1.15$ . These parameters were chosen to make easier the comparison between different domains.

#### 3.1 Confocal elliptical cylinders

We start by presenting the heat conduction problem in the gap between two confocal elliptical cylinders. This case was already solved in [37], but we summarize it here for completeness. This is the first example in literature of truly bi-dimensional problem in extended thermodynamics and it is the first natural extension of

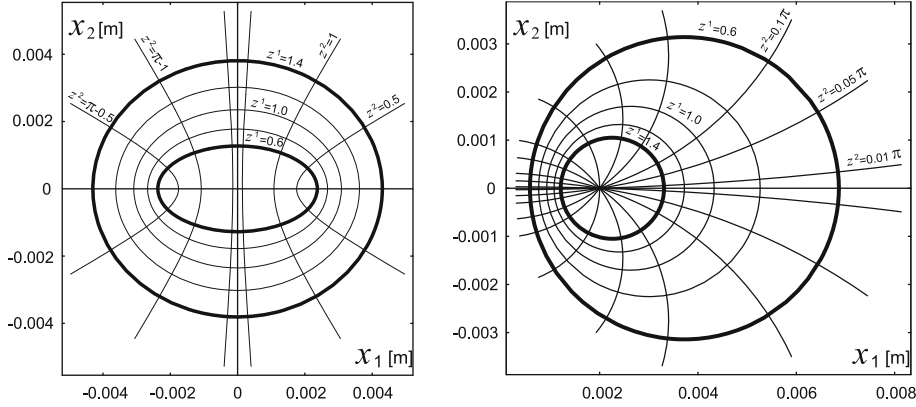


**Fig. 1** A sketch of the coordinates considered in this paper. **a** Elliptic-hyperbolic coordinates. **b** Bi-cylindrical coordinates

the case of two coaxial cylinders, already studied in [35]. In this case, the most suitable coordinates are the elliptic-hyperbolic ones  $(z^1, z^2, z^3)$ , known also as the elliptic cylindrical coordinates, which are related to the cartesian ones  $(x_1, x_2, x_3)$  by [37,41]

$$\begin{aligned} x_1 &= c \cosh z^1 \cos z^2, \\ x_2 &= c \sinh z^1 \sin z^2, \\ x_3 &= z^3, \end{aligned} \quad (19)$$

where

$$z_i^1 \leq z^1 \leq z_e^1, \quad 0 \leq z^2 < 2\pi, \quad -\infty < z^3 < \infty. \quad (20)$$

The coordinate surfaces are

$$\begin{aligned} \frac{x_1^2}{\cosh^2 z^1} + \frac{x_2^2}{\sinh^2 z^1} &= c^2, \\ \frac{x_1^2}{\cos^2 z^2} - \frac{x_2^2}{\sin^2 z^2} &= c^2, \\ x_3 &= z^3. \end{aligned} \quad (21)$$

In Fig. 1a, the ellipses and hyperbolae are the intersections of the first two families with the plane  $x_3 = 0$ . It is easy to ascertain that in this geometry the length  $2c$  represents the distance between the foci of the ellipses and of the hyperbolae. With respect to these coordinates, the metric tensor is diagonal and the following relations hold:

$$\begin{aligned} g &= \frac{2}{c^2} \frac{1}{\cosh 2z^1 - \cos 2z^2}, \quad g^{33} = 1, \\ \Gamma_{11}^1 &= \frac{\sinh 2z^1}{\cosh 2z^1 - \cos 2z^2}, \quad \Gamma_{22}^2 = \frac{\sin 2z^2}{\cosh 2z^1 - \cos 2z^2}, \quad \Gamma_{31}^3 = \Gamma_{32}^3 = 0. \end{aligned} \quad (22)$$

If both boundary cylinders are kept at different constant temperatures— $\tilde{T}_e = 1$  at the external cylinder  $z_e^1 = 1.4$  and  $\tilde{T}_i = 1.15$  at the inner cylinder  $z_i^1 = 0.6$ —the problem of heat conduction reduces to the integration of an ordinary differential equation. In fact, due to the symmetry of the domain and of the boundary data, it is possible to assume that the temperature does not depend on  $z^2$  and  $z^3$ . In this manner, Eq. (18)<sub>2</sub>, which is usually very complicated to be integrated, reduces to the trivial form:

$$\frac{d^2 \tilde{T}}{(dz^1)^2} = 0. \quad (23)$$

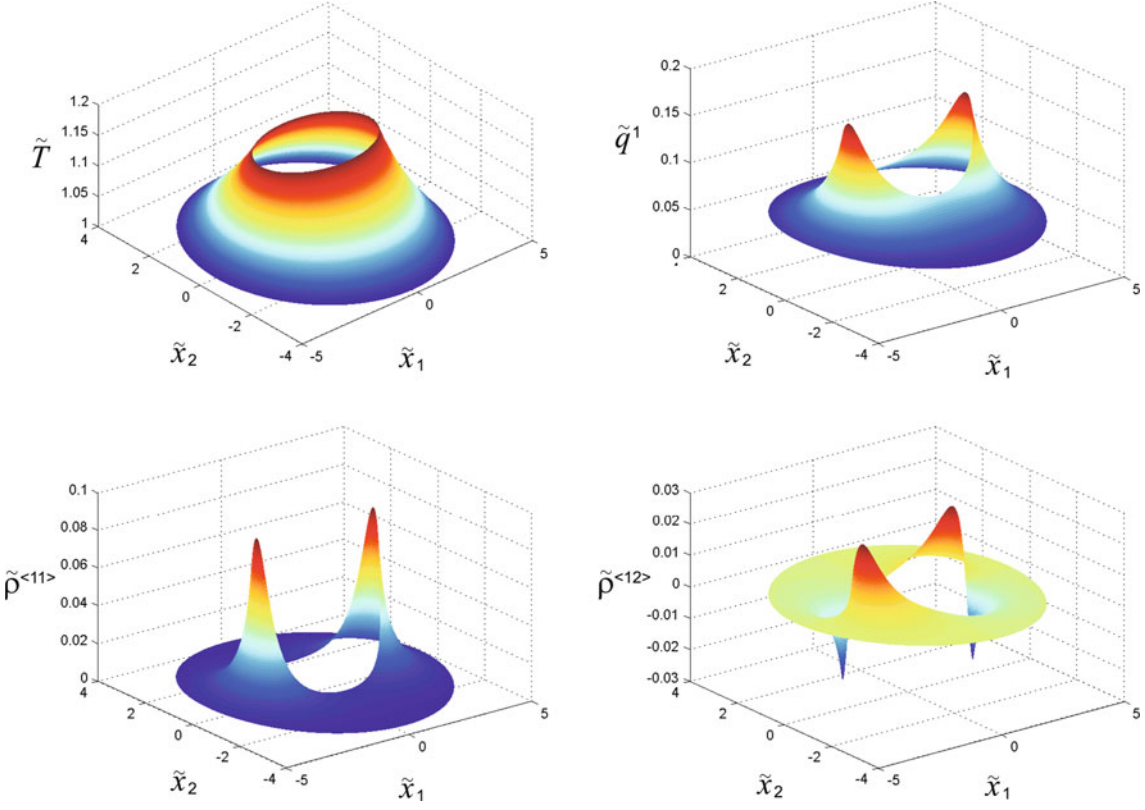


**Fig. 2** The case of elliptical confocal cylinders

Then, from Eqs. (18) and (23), we easily get the analytical solution of the problem:

$$\begin{aligned}
\tilde{T} &= \tilde{T}_i + \frac{\tilde{T}_e - \tilde{T}_i}{z_e^1 - z_i^1} (z^1 - z_i^1), \\
\tilde{q}^1 &= -\frac{5}{2} Kn \sqrt{\tilde{g}} \frac{\tilde{T}_e - \tilde{T}_i}{z_e^1 - z_i^1}, \\
\tilde{q}^2 &= 0, \\
\tilde{\rho}^{(11)} &= -\tilde{\rho}^{(22)} = -2Kn^2 \tilde{g} \Gamma_{11}^1 \frac{\tilde{T}_e - \tilde{T}_i}{z_e^1 - z_i^1}, \\
\tilde{\rho}^{(12)} &= -2Kn^2 \tilde{g} \Gamma_{22}^2 \frac{\tilde{T}_e - \tilde{T}_i}{z_e^1 - z_i^1}; 
\end{aligned} \tag{24}$$

whose behavior is shown in Fig. 2 in terms of  $\tilde{x}_1 = 2x_1/c$  and  $\tilde{x}_2 = 2x_2/c$ .

We notice that whereas  $\tilde{T}$ ,  $\tilde{q}^1$  and  $\tilde{q}^2 = 0$  are the same as those predicted by the Fourier law, the two normal and the shear components of the deviatoric pressure tensor do not vanish, in contrast to the Navier–Stokes law. Clearly, the differences between the classical and the Grad theory are more remarkable around the major axis of the ellipses, where the curvature is larger.

### 3.2 Non-coaxial circular cylinders

Another way to obtain a pure bi-dimensional problem from that of the two coaxial circular cylinders is to make them non-coaxial. This is the second problem that we will present in this chapter.

In order to describe heat conduction between two non-coaxial circular cylinders, we refer to the bi-cylindrical coordinates  $(z^1, z^2, z^3)$  [41] – known also as bipolar cylindrical coordinates – defined in

$$z_e^1 \leq z^1 \leq z_i^1, \quad 0 \leq z^2 < 2\pi, \quad -\infty < z^3 < \infty. \quad (25)$$

The relations between such coordinates and the cartesian ones read

$$x_1 = c \frac{\sinh z^1}{\cosh z^1 - \cos z^2}, \quad x_2 = c \frac{\sin z^2}{\cosh z^1 - \cos z^2}, \quad x_3 = z^3. \quad (26)$$

The corresponding coordinate surfaces are expressed by

$$\begin{aligned} (x_1 - c \coth z^1)^2 + x_2^2 &= c^2 (\coth^2 z^1 - 1), \\ x_1^2 + (x_2 - c \cot z^2)^2 &= c^2 (\cot^2 z^2 + 1), \\ x_3 &= z^3, \end{aligned} \quad (27)$$

where the first two families represent right circular cylinders with element parallel to the  $x_3$ -axis. Their intersection with the plane  $x_3 = 0$  is shown in Fig. 1b. The quantity  $c$  is related to the radii of the internal and external circles –, respectively,  $a = c / \sinh z_i^1$  and  $b = c / \sinh z_e^1$  – and the distance  $d$  between their centers by the relation

$$c^2 = \frac{1}{4d^2} [(d^2 - a^2 - b^2)^2 - 4a^2b^2]. \quad (28)$$

With respect to these coordinates, the metric tensor and the Christoffel symbols in (9) are given by

$$\begin{aligned} g &= \frac{(\cos z^2 - \cosh z^1)^2}{c^2}, \quad g^{33} = 1, \\ \Gamma_{11}^1 &= \frac{\sinh z^1}{\cos z^2 - \cosh z^1}, \quad \Gamma_{22}^2 = \frac{\sin z^2}{\cos z^2 - \cosh z^1}, \quad \Gamma_{31}^3 = \Gamma_{32}^3 = 0. \end{aligned} \quad (29)$$

As in Sect. 3.1, we assume that both boundary cylinders are kept at different constant temperatures: the external cylinder,  $z_e^1 = 0.6$ , is kept at the temperature  $\tilde{T}_e = 1$ , while the inner one, corresponding to  $z_i^1 = 1.4$ , is kept at  $\tilde{T}_i = 1.15^2$ . As in the previous case, the problem can be described with an ordinary differential equation and the Laplace equation assumes again the form (23). For this reason, the solution for non-coaxial circular cylinders coincides formally with the solution of confocal elliptical cylinders (24). Clearly, there are still some differences, due to the different expressions of the metric tensor and of the Christoffel symbols. The solution for this problem is shown in Fig. 3. Also for this domain  $\tilde{T}$ ,  $\tilde{q}^1$  and  $\tilde{q}^2 = 0$  coincide with those predicted by the Fourier law. The differences between the classical and the linearized 13-moment theory can be found in the non-vanishing components of the deviatoric pressure tensor. Obviously, the most evident variances have to be sought in the region where the two cylinders are closer. In fact, in this region, we expect steeper gradients that can be better described by extended thermodynamics.

### 3.3 Confocal ellipsoids

Now we refer to a bi-dimensional problem related to the heat conduction between two concentric spheres already studied in [35]. The most natural way is to deform the two spheres into two confocal ellipsoids.

The suitable coordinates for the description of heat conduction between two confocal ellipsoids turn out to be the prolate spheroidal coordinates  $(z^1, z^2, z^3)$  defined in

$$\begin{aligned} z_i^1 &\leq z^1 \leq z_e^1, \\ 0 &\leq z^2 < 2\pi, \\ 0 &\leq z^3 < \pi. \end{aligned} \quad (30)$$

<sup>2</sup> It is important to stress that, due to the definition of the bi-cylindrical coordinates, increasing values of  $z^1$  correspond to cylinders with decreasing radii.

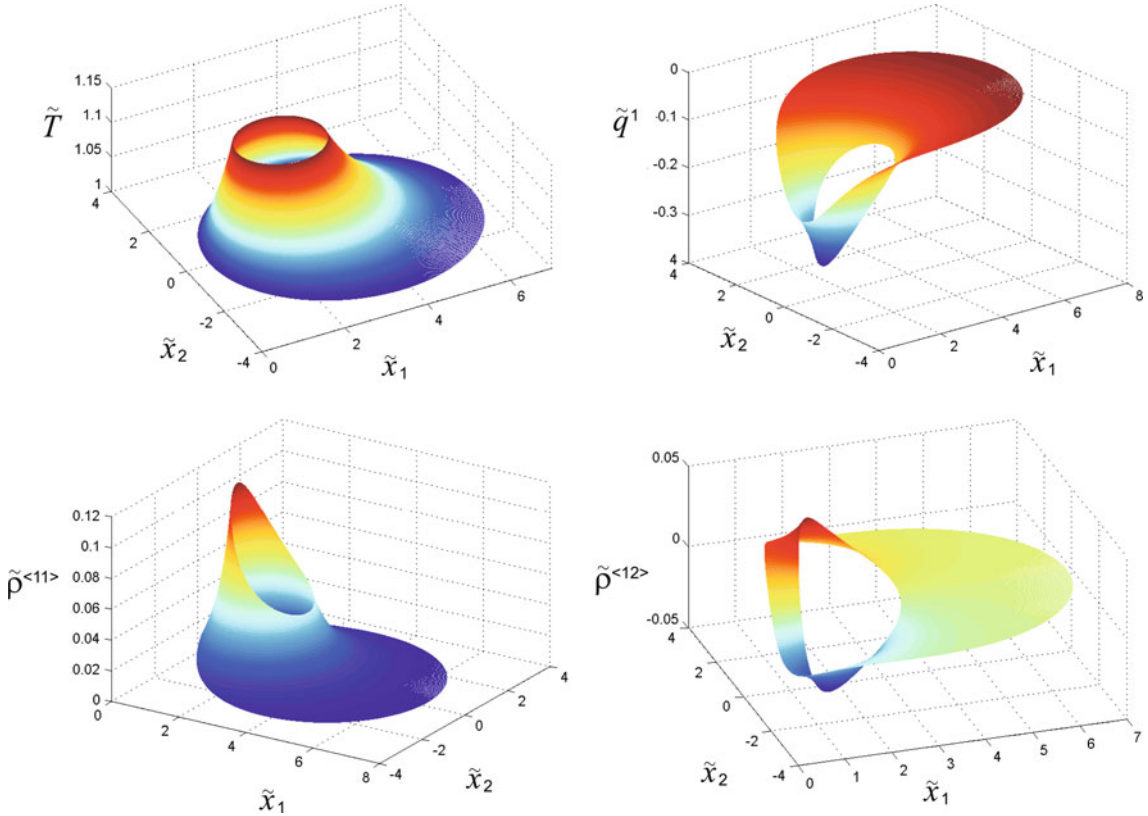


**Fig. 3** The case of non-coaxial circular cylinders

For them it holds [41]

$$\begin{aligned} x_1 &= c \cosh z^1 \cos z^2, \\ x_2 &= c \sinh z^1 \sin z^2 \sin z^3, \\ x_3 &= c \sinh z^1 \sin z^2 \cos z^3. \end{aligned} \quad (31)$$

In this case, the coordinate surfaces are

$$\begin{aligned} \frac{x_1^2}{\cosh^2 z^1} + \frac{x_2^2 + x_3^2}{\sinh^2 z^1} &= c^2, \\ \frac{x_1^2}{\cos^2 z^2} - \frac{x_2^2 + x_3^2}{\sin^2 z^2} &= c^2, \\ x_2 &= x_3 \tan z^3. \end{aligned} \quad (32)$$

The first two relations represent respectively a family of ellipsoids and hyperboloids of revolution generated by the rotation of the ellipses and of the hyperbolae shown in Fig. 1a around the  $x_1$ -axis. The third coordinate surfaces are planes including the  $x_1$ -axis and forming an angle  $z^3$  with the positive  $x_3$ -axis. Here the quantity  $c$  has exactly the same role as in Sect. 3.2. With respect to these coordinates, the metric tensor and the Christoffel symbols read

$$\begin{aligned} g &= \frac{2}{c^2} \frac{1}{\cosh 2z^1 - \cos 2z^2}, & g^{33} &= \frac{1}{c^2 \sinh^2 z^1 \sin^2 z^2}, \\ \Gamma_{11}^1 &= \frac{\sinh 2z^1}{\cosh 2z^1 - \cos 2z^2}, & \Gamma_{22}^2 &= \frac{\sin 2z^2}{\cosh 2z^1 - \cos 2z^2}, \\ \Gamma_{31}^3 &= \coth z^1, & \Gamma_{32}^3 &= \cot z^2. \end{aligned} \quad (33)$$

As previously said, we are interested in heat conduction between two ellipsoids kept at two different constant temperatures with the usual boundary data—that are  $\tilde{T}_e = 1$  at  $z_e^1 = 1.4$  and  $\tilde{T}_i = 1.15$  at  $z_i^1 = 0.6$ . Then, also in the case of two ellipsoids, the problem comes down to the study of the behavior of the temperature as a function of only a variable, i.e. the  $z_1$ -coordinate. In this way, Eq. (18)<sub>2</sub> reduces to a simpler form:

$$\frac{d^2\tilde{T}}{d(z^1)^2} + \coth z^1 \frac{d\tilde{T}}{dz^1} = 0, \quad (34)$$

whose solution is

$$\tilde{T}(z^1) = \frac{\tilde{T}_e \ln \left( \tanh \frac{z_e^1}{2} \coth \frac{z_i^1}{2} \right) - \tilde{T}_i \ln \left( \tanh \frac{z_e^1}{2} \coth \frac{z_e^1}{2} \right)}{\ln \left( \tanh \frac{z_e^1}{2} \coth \frac{z_i^1}{2} \right)}. \quad (35)$$

Inserting Eq. (35) into Eqs. (18)<sub>3–7</sub>, we retrieve the explicit expression for the other fields, i.e.

$$\begin{aligned} \tilde{q}^1 &= -\frac{5}{2} Kn \sqrt{\tilde{g}} A, \\ \tilde{q}^2 &= 0, \\ \tilde{\rho}^{(11)} &= -2Kn^2 \tilde{g} (\coth z_1 + \Gamma_{11}^1) A, \\ \tilde{\rho}^{(12)} &= -2Kn^2 \tilde{g} \Gamma_{22}^2 A, \\ \tilde{\rho}^{(22)} &= 2Kn^2 \tilde{g} \Gamma_{11}^1 A, \\ \text{with } A &= \frac{\tilde{T}_e - \tilde{T}_i}{\sinh z_1 \ln \left( \tanh \frac{z_e^1}{2} \coth \frac{z_i^1}{2} \right)}. \end{aligned} \quad (36)$$

These solutions are illustrated in Fig. 4.

Also in this geometry  $\tilde{T}$ ,  $\tilde{q}^1$  and  $\tilde{q}^2 = 0$  coincide with those predicted by the Fourier law and we have non-vanishing  $\tilde{\rho}^{(ij)}$ . It is clear that these results for the ellipsoids are similar to those obtained for the confocal elliptical cylinders. This fact is a consequence of the geometry of the both problems and of the similarity of the coordinates we have chosen to describe the domains. As in the case of confocal elliptical cylinders, the most significant differences between NSF model and the linearized 13-moment equations can be found in the values of  $\tilde{\rho}^{(ij)}$  along the major axes of the ellipses. In addition to the previous case, here we have  $\tilde{\rho}^{(11)} \neq -\tilde{\rho}^{(22)}$  and consequently a non-vanishing  $\tilde{\rho}^{(33)}$  component of the stress tensor.

A comparison of the results of Sects. 3.1 and 3.3 is presented in Fig. 5 through two bi-dimensional pictures of  $\tilde{\rho}^{(11)}$  along the major semi-axis of the ellipses, characterized by  $z^2 = 0$ , and around the inner ellipse, where  $z^1 = 0.6$  (that are the coordinates lines where the deviatoric stress tensor reaches its highest values). This figure shows that the values of  $|\tilde{\rho}^{(ij)}|$  are greater for the ellipsoids than for the elliptical cylinders.

### 3.4 Non-concentric spheres

The last problem we present is the heat conduction between two non-concentric spheres. In this case, it is appropriate to refer to the bi-spherical coordinates related to the cartesian ones by

$$\begin{aligned} x_1 &= c \frac{\sinh z^1}{\cosh z^1 - \cos z^2}, \\ x_2 &= c \frac{\sin z^2 \sin z^3}{\cosh z^1 - \cos z^2}, \\ x_3 &= c \frac{\sin z^2 \cos z^3}{\cosh z^1 - \cos z^2}, \end{aligned} \quad (37)$$

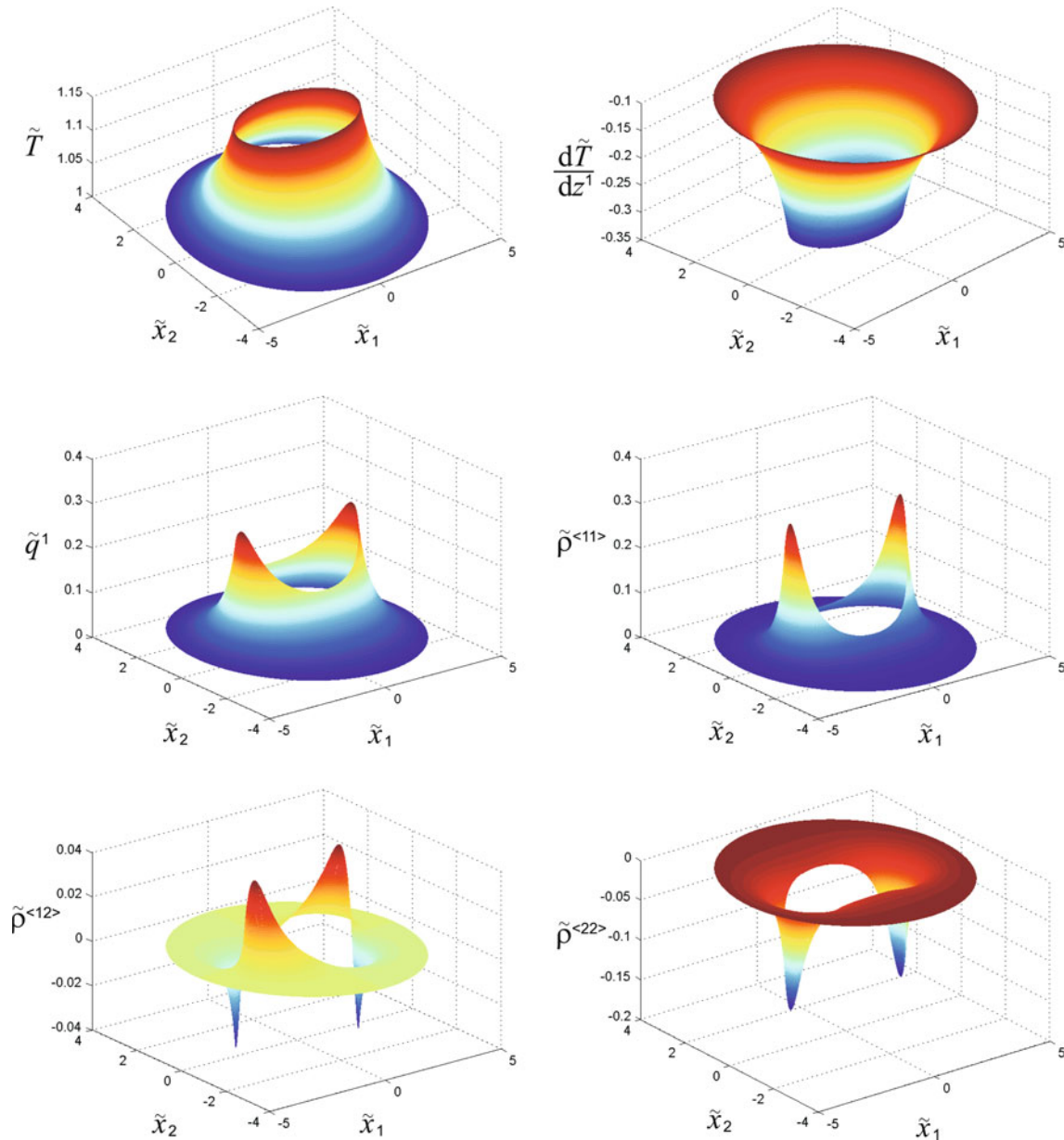


**Fig. 4** The case of two confocal ellipsoids

where

$$\begin{aligned} z_e^1 &\leq z^1 \leq z_i^1, \\ 0 &\leq z^2 < 2\pi, \\ 0 &\leq z^3 < \pi. \end{aligned} \tag{38}$$

Hence, the corresponding coordinate surface are described by

$$\begin{aligned} (x_1 - c \coth z^1)^2 + x_2^2 + x_3^2 &= c^2 (\coth^2 z^1 - 1), \\ x_1^2 + (\sqrt{x_2^2 + x_3^2} - c \cot z^2)^2 &= c^2 (\cot^2 z^2 + 1), \\ x_2 &= x_3 \tan z^3, \end{aligned} \tag{39}$$

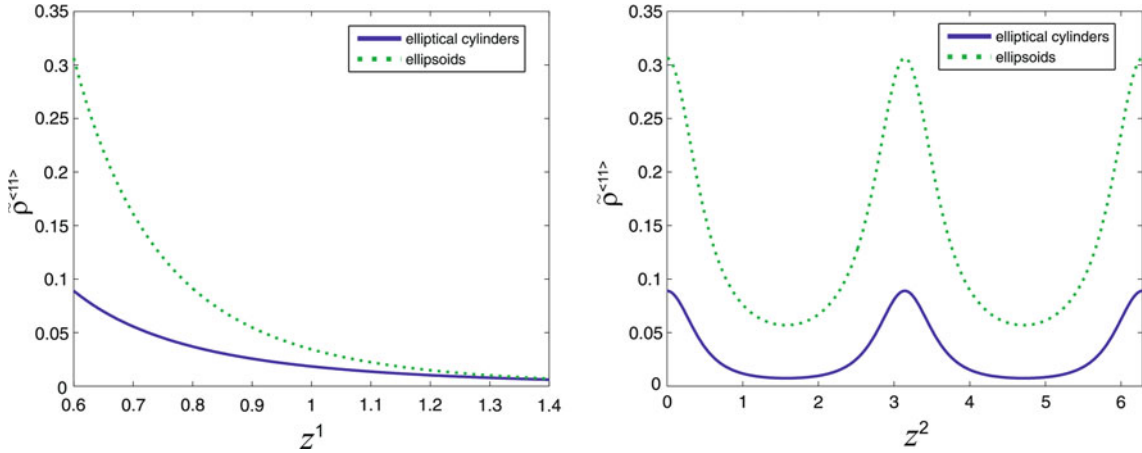


**Fig. 5** Comparison between elliptical cylinders and ellipsoids

that are spheres, obtained by the revolution of the circles in Fig. 1b around the  $x_1$ -axis, and planes containing the  $x_1$ -axis. In this case the metric tensor and the Christoffel symbols of (9) read

$$\begin{aligned} g &= \frac{(\cos z^2 - \cosh z^1)^2}{c^2}, & g^{33} &= \frac{(\cos z^2 - \cosh z^1)^2}{c^2 \sin^2 z^2}, \\ \Gamma_{11}^1 &= \Gamma_{31}^3 = \frac{\sinh z^1}{\cos z^2 - \cosh z^1}, & \Gamma_{22}^2 &= \frac{\sin z^2}{\cos z^2 - \cosh z^1}, \\ \Gamma_{32}^3 &= -\frac{\cos z^2 \cosh z^1 - 1}{(\cos z^2 - \cosh z^1) \sin z^2}. \end{aligned} \quad (40)$$

We assume that the two boundary spheres are kept at the usual constant temperatures  $-\tilde{T}_e = 1$  at  $z_e^1 = 0.6$  and  $\tilde{T}_i = 1.15$  at  $z_i^1 = 1.4$ . Then, differently from the other cases, in this geometry the solution for the temperature must depend on both the variables  $z^1$  and  $z^2$ . In fact, the Laplace equation (18)<sub>2</sub> in the bi-spherical coordinates assumes the form

$$\frac{\partial}{\partial z^1} \left( \frac{\sin z^2}{\cos z^2 - \cosh z^1} \frac{\partial \tilde{T}}{\partial z^1} \right) + \frac{\partial}{\partial z^2} \left( \frac{\sin z^2}{\cos z^2 - \cosh z^1} \frac{\partial \tilde{T}}{\partial z^2} \right) = 0, \quad (41)$$

and it is not possible to neglect the dependence of the temperature on the  $z^2$ -coordinate. Fortunately, Eq. (41) can still be solved analytically through the method of variable separation and by suitable orthogonal functions [41]. Thus, the solution is

$$\tilde{T} = \tilde{T}_e + \sqrt{2}(\tilde{T}_i - \tilde{T}_e)\sqrt{\cosh z^1 - \cos z^2} \sum_{n=0}^{\infty} P_n(\cos z^2) e^{-(n+\frac{1}{2})z_i^1} \frac{\sinh((n+\frac{1}{2})(z^1 - z_e^1))}{\sinh((n+\frac{1}{2})(z_i^1 - z_e^1))}, \quad (42)$$

where  $P_n$  denotes the Legendre polynomial of order  $n$ . After some calculations, it is easy to deduce from (18) explicit analytical expressions for all the field variables.

In Fig. 6, the behavior of the field variables in the case of non-concentric spheres is shown. It is important to stress that a good approximation to the solution (42) is obtained by truncating the series to the first 30 terms. This approximation is used for the graphics together with the properties of Legendre polynomial derivatives. The case of non-concentric spheres differs from all the previous ones since the problem cannot be studied in a one-dimensional space, and this property implies, in particular, that  $\tilde{\rho}^2$  does not vanish anymore.

The geometry of the domains and the expression of the bi-cylindrical and bi-spherical coordinates suggest a comparison between the cases illustrated in Sects. 3.2 and 3.4. To this aim, we refer to Fig. 7 in which the behavior of  $\tilde{\rho}^{(11)}$  between the centers – where  $z^2 = \pi$  – and around the internal cylinder or sphere (i.e. at  $z^1 = 1.4$ ) is displayed. It turns out that for the spheres the values of  $|\tilde{\rho}^{(ij)}|$  are higher than those of the circular cylinders.

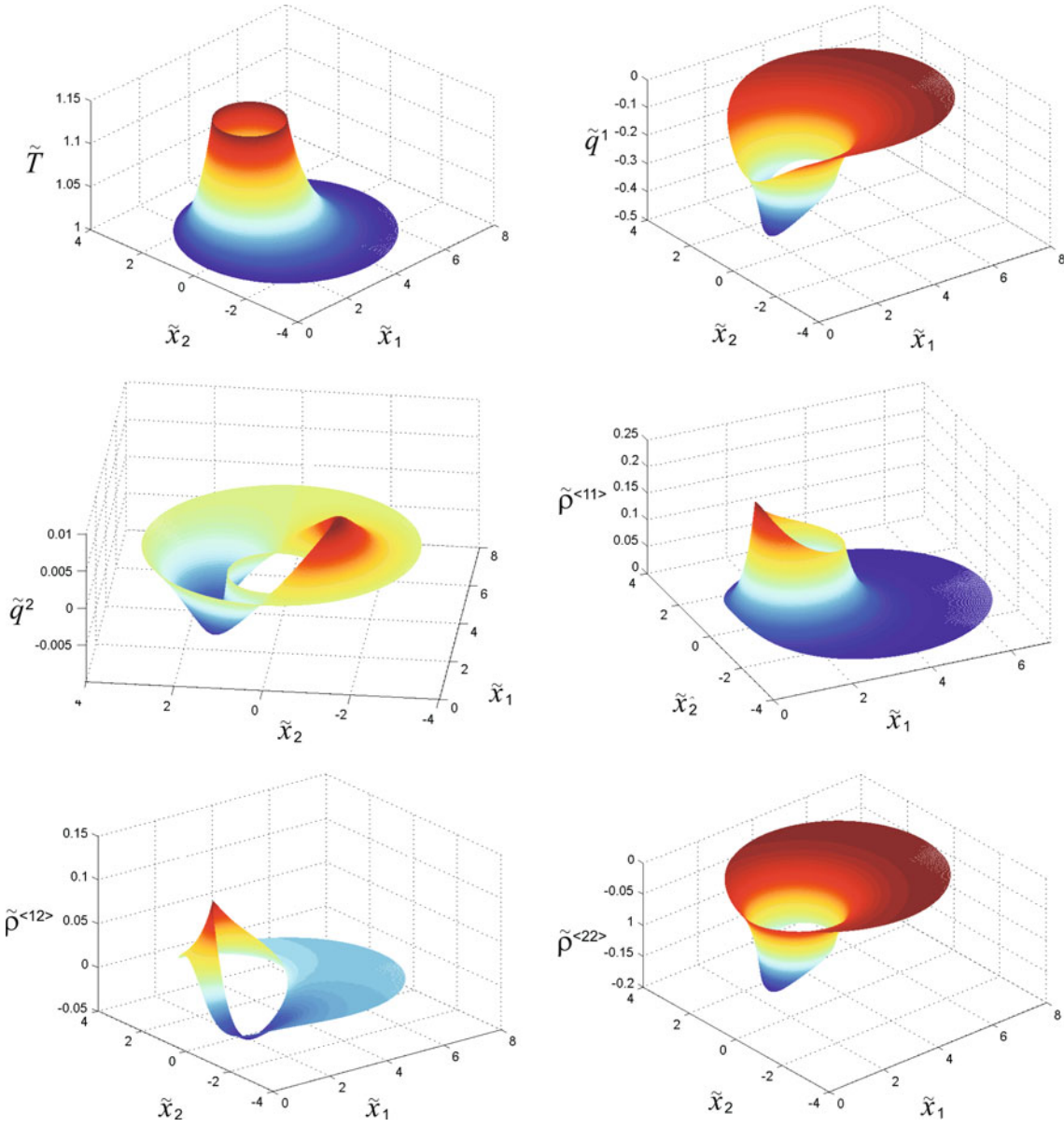


**Fig. 6** The case of two non-concentric spheres

#### 4 The role of the Knudsen number

We are now interested in the dependence of the solutions on the rarefaction of the gas and, as already said, the Knudsen number can be viewed as an index of the gas rarefaction. For this reason, in this section we investigate the behavior of the solutions when the values of  $Kn$  are varied. More precisely, in Fig. 8 we have shown the field  $\tilde{\rho}^{(11)}$  for different values of  $Kn$  in the cases of confocal ellipsoids and non-concentric spheres. In particular, for the confocal ellipsoids,  $\tilde{\rho}^{(11)}$  is shown in Fig. 8a along the major semi-axis of the ellipses ( $z^2 = 0$ ), while in Fig. 8b at the inner ellipse ( $z^1 = 0.6$ ); for the case of the non-concentric spheres  $\tilde{\rho}^{(11)}$  is illustrated in Fig. 8c along the distance between the centers of the two circles ( $z^2 = \pi$ ) and in Fig. 8d at the internal hole ( $z^1 = 1.4$ ).

From Fig. 8, it is evident that the more rarefied is the gas, the greater are the differences between classical and extended thermodynamics. Indeed, the greater is the value of  $Kn$ , the higher is the value of  $\rho^{(11)}$ . We can consider  $\rho^{(11)}$  as a “measure” of the validity of the classical thermodynamics, in the sense that if this field component is close to 0, the agreement between NSF and Grad’s theory is very good.

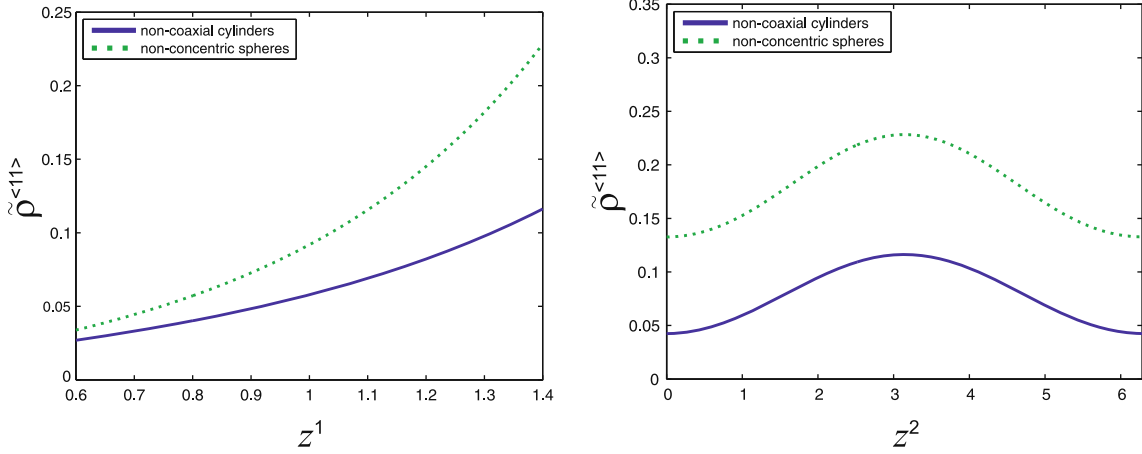


**Fig. 7** A comparison between non-coaxial circular cylinders and non-concentric spheres with regard to  $\tilde{\rho}^{(11)}$

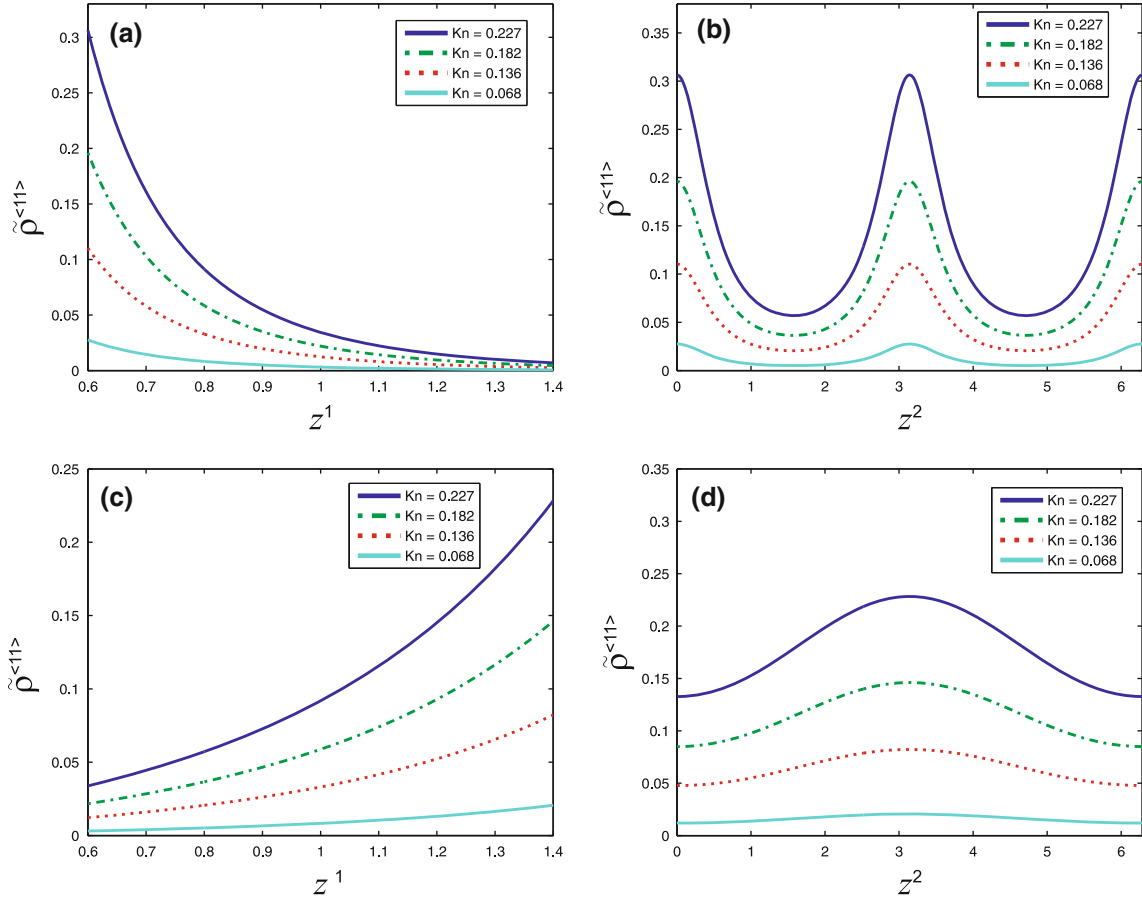


**Fig. 8** The role of  $Kn$  illustrated through  $\tilde{\rho}^{(11)}$ . **a, b** The case of confocal ellipsoids, **c, d** the case of non-concentric spheres

## 5 Non-equilibrium temperature

In this section, we define a non-equilibrium temperature for the problems previously studied.

We follow the definition of non-equilibrium temperature presented in [40], which has been employed in [42] for a stationary problem in a gas described by extended thermodynamics with 14 moments, and used in [35, 37] in the context of extended thermodynamics with 13 moments in curved domains:

The kinetic theory of gases, if exploited close to equilibrium, introduces the temperature as a measure of the mean kinetic energy of the atoms. In fact, in the previous sections, we have referred to this definition and, for this reason,  $T$  was called the *kinetic temperature*.

In non-equilibrium, we introduce the temperature  $t$  as the factor of proportionality between the entropy flux  $\phi^k$  and the heat flux  $q^k$ , that is

$$\phi^k = \frac{1}{t} q^k. \quad (43)$$

The energy conservation guarantees that the normal component of  $q^k$  is continuous at a wall (or at the surfaces of separation of two bodies) and we expect that a wall does not produce entropy; hence it is reasonable to suppose that the normal component of  $\phi^k$  is also continuous. From (43), it follows that also  $t$  should be continuous.

The continuity of  $t$  makes this so-called *thermodynamic* temperature a field that can be measured by a thermometer in accordance with the zeroth law of thermodynamics, which defines the temperature as the quantity continuous across a wall or a surface of separation between two bodies.

In extended thermodynamics, a special effort was made to compare these two temperatures, see for example [40, 42, 43]. A first difference between  $T$  and  $t$  in the 13-moment theory was pointed out by Müller and Ruggeri in [35] for the heat conduction between coaxial cylinders or concentric spheres. Then, Barbera and Müller [37] showed that these two temperatures are also different in the case of two confocal elliptical cylinders. In our cases, there are also some differences between  $T$  and  $t$ , as we are going to show.

In the 13-moment theory, the entropy flux is expressed in terms of the heat flux by<sup>3</sup> [3]

$$\phi^k = \frac{1}{T} \left( q^k - \frac{2}{5} \frac{\rho^{(kj)}}{p_0} g_{ji} q^i \right). \quad (44)$$

From (43) and (44), it is evident that the presence of non-vanishing traceless parts of the stress tensor gives rise to differences between the kinetic and the non-equilibrium temperatures. For a gas at rest, in the NSF theory the stress tensor vanishes and no differences between the two temperatures is observable.

On the contrary, in our ET model, in spite of the linearization, we have still some non-vanishing components of  $\rho^{(ik)}$ , and those components make the difference.

In order to derive explicitly a relation between  $T$  and  $t$ , the first three geometries (Sects. 3.1–3.3) can be treated together. In fact, in those cases there is only one non-vanishing component of the heat flux, that is  $q^1$ , so the entropy flux and the heat flux are parallel vectors, both normal to the boundary surfaces. Then, relation (44) becomes

$$\phi^1 = \frac{1}{T} \left( 1 - \frac{2}{5} \frac{\rho^{(11)}}{p_0} \frac{1}{g} \right) q^1, \quad (45)$$

and comparison of (45) with (43) and relations (12) and (14) yield

$$\frac{t}{T} = \frac{1}{1 - \frac{2}{5} \tilde{\rho}^{(11)}}. \quad (46)$$

The ratio between the two temperatures is illustrated in Fig. 9a–c, for the parameter values and the boundary data already assigned in Sect. 3. It must be recalled that the ratio  $t/T$  in the case of elliptical cylinders was already determined in [37].

For the case of non-concentric spheres, the heat flux has two non-vanishing components, i.e.  $q^1$  and  $q^2$ , hence, the entropy flux and the heat flux are no more parallel. Nevertheless, for the continuity property, we are interested only in the flux components normal to the boundary spheres and we define as non-equilibrium temperature the ratio between the first component of the heat flux and the first component of the entropy flux. From (44), we get

$$\phi^1 = \frac{1}{T} \left[ \left( 1 - \frac{2}{5} \frac{\rho^{(11)}}{p_0} \frac{1}{g} \right) q^1 - \frac{2}{5} \frac{\rho^{(12)}}{p_0} \frac{1}{g} q^2 \right], \quad (47)$$

<sup>3</sup> In (44) we have considered the second order terms. In fact, even in the linearized theory, the entropy inequality and therefore the heat flux must contain the non-linear terms, otherwise it loses all the meaning.

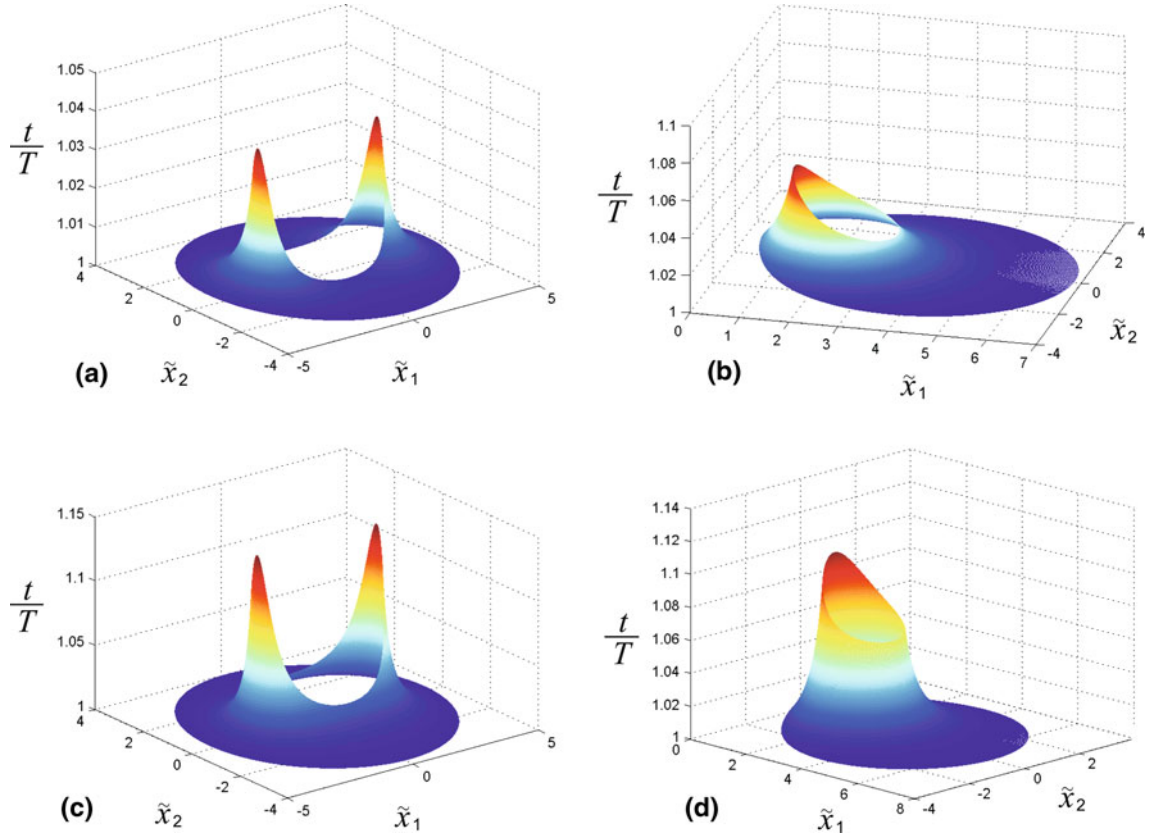


**Fig. 9** The ratio between the non-equilibrium  $t$  and the kinetic  $T$  temperatures for: **a** confocal elliptical cylinder; **b** non-coaxial circular cylinders; **c** confocal ellipsoids; **d** non-concentric spheres

and therefore, in this case we have

$$\frac{t}{T} = \frac{1}{1 - \frac{2}{5}\tilde{\rho}^{(11)} - \frac{2}{5}\tilde{\rho}^{(12)}\frac{\tilde{q}^2}{\tilde{q}^1}}. \quad (48)$$

This ratio is presented in Fig. 9d.

From Figs. 9a and c, we can conclude that in the cases of confocal elliptical cylinders and ellipsoids the two temperatures differ mostly along the major axes of the ellipses near the inner one. This reflects the behavior of the field  $\tilde{\rho}^{(11)}$ . Clearly, the ratio between the two temperatures is greater in the case of the confocal ellipsoids. Figs. 9b and d show that the differences between  $T$  and  $t$  increase in the region where the two circles are closer, exactly where the gradient are greater. Here, the ratio  $t/T$  is greater in the case of the spheres, due to both the geometry of the problem and the additional term in (48) containing the deviatoric part of the stress tensor,  $\tilde{\rho}^{(12)}$ .

The definition of the temperature out of equilibrium is a controversial point and has been subject of a large number of studies, see, for example, the references related to extended thermodynamics [35, 37, 40, 42–46]. We have shown here that in the heat conduction problem it is possible to observe differences between the kinetic and the non-equilibrium temperature, also when a fixed value of the kinetic temperature is prescribed at the boundary. How to integrate the equations with a fixed value of  $t$  on the boundary is still an open question for the cases we have presented in the previous sections.

## 6 Remarks about the linearization

Concerning the validity of the linearization proposed in Sect. 2, we want to make some remarks. First of all, it can be easily verified that the results presented in this paper are in agreement with the assumptions made for the linearization (i.e.  $\tilde{\rho}^{(ij)}$ , the heat fluxes and the spatial derivatives of the kinetic temperature are “small”).

Moreover, we have compared the solutions of the non-linear model and the linearized one in the case of heat conduction between two concentric cylinders; that is to say, in a case already known in the literature [35] for which it is possible to write the explicit solution of the non-linear model. For the same parameter values and the same boundary data as in Sect. 3, it turns out that the solutions are very close together. This fact confirms the idea that, for suitable parameters and boundary value choices, the linearization is correct. Obviously, for phenomena further from the equilibrium, this kind of approximation is no more valid.

## 7 Conclusions and final remarks

In this paper, we have studied the stationary heat conduction problem in a classical monatomic ideal gas at rest and compared the solutions of rational extended thermodynamics [3] with that of classical thermodynamics. We have extended the results previously obtained in [35,37] to any problem of stationary heat conduction in a gas at rest confined in a curved domain, described by orthogonal coordinates satisfying few properties. In particular, in Sect. 2 the complete set of equations and the linearized ones are presented. In fact, in order to determine all the solutions analytically, we have simplified the model, considering the linearized equations of extended thermodynamics with 13 moments, as already done in [37] for the case of elliptical cylinders.

Due to the linearization, the temperature behavior is the one predicted by Fourier law, but also for this very simple linearized theory, there are non-vanishing components of the stress tensor, in contrast to Navier–Stokes equations. These results are obtained for different geometries (we have analyzed here 4 different cases, 3 of them were never studied before) and referring to them, we presuppose that *the stress tensor does not vanish for any heat conduction problem in a gas at rest confined in a curved domain*.

An important final remark concerns the non-linearized 13-moment system described at the beginning of this paper. As already said, it cannot easily be solved analytically, but it seems that, far from the equilibrium state, other interesting results are to be expected. The non-linear effects are already under investigation and they will be part of a further work.

**Acknowledgments** This paper was supported by GNFM-INdAM and partially by the GNFM project “Progetto giovani ricercatori 2008: Metodi analitici e numerici per lo studio di modelli classici e quantistici in Termodinamica Estesa e per l’analisi della stabilità in fluidodinamica”.

## References

1. Eckart, C.: The thermodynamics of irreversible processes I: The simple fluid. *Phys. Rev.* **58**, 267–269 (1940)
2. Müller, I.: *A History of Thermodynamics*. Springer, Berlin (2007)
3. Müller, I., Ruggeri, T.: *Rational Extended Rational Thermodynamics*. Springer, New York (1998)
4. Meixner, J.: Zur Thermodynamik irreversibler Prozesse in Gasen mit chemisch reagierenden, dissoziierenden und anregbaren Komponenten. *Ann. Phys.* **43**, 244–270 (1943)
5. Prigogine, I.: *Introduction to Thermodynamics of Irreversible Processes*. Interscience, New York (1961)
6. De Groot, S.R., Mazur, P.: *Non-equilibrium Thermodynamics*. North-Holland, Amsterdam (1962)
7. Truesdell, C.: *Rational Thermodynamics* (2nd ed.). Springer, New York (1984)
8. Colemann, B.D., Markovitz, H., Noll, W.: *Viscometric Flows of Non-Newtonian Fluids*. Springer, New York (1966)
9. Müller, I.: Zum Paradox der Wärmeleitungstheorie. *Z. Phys.* **198**, 329–344 (1967)
10. Liu, I.S.: Method of lagrange multipliers for exploitation of the entropy principle. *Arch. Rational Mech. Anal.* **46**, 131 (1972)
11. Boillat, G.: Sur l’existence et la recherche d’équations de conservation supplémentaires pour les systèmes hyperboliques. *C.R. Acad. Sc. Paris* **278**(A), 909 (1974)
12. Ruggeri, T., Strumia, A.: Main field and convex covariant density for quasi-linear hyperbolic systems. Relativistic fluid dynamics. *Ann. Inst. H. Poincaré* **34**(A), 65 (1981)
13. Grad, H.: On the kinetic theory of rarefied gases. *Comm. Pure Appl. Math.* **2**, 331–407 (1949)
14. Grad H.: Principles of the Kinetic Theory of Gases. In: Flügge, S (ed.) *Handbuch der Physik XII*, pp. 205–294. Springer-Verlag, Heidelberg (1958)
15. Jou, D., Casas-Vázquez, J., Lebon, G.: *Extended Irreversible Thermodynamics*. Springer, Berlin (2001)
16. Jou, D., Casas-Vázquez, J., Criado-Sancho, M.: *Thermodynamics of Fluids Under Flow*. Springer, Berlin (2000)
17. Nettleton, R.E., Sobolev, S.L.: Applications of Extended Thermodynamics to chemical, rheological and transport processes: A special survey I and II. *J. Non Equilib. Thermodyn.* **20**, 205–229 and 297–331 (1995)
18. Nettleton, R.E., Sobolev, S.L.: Applications of extended thermodynamics to chemical, rheological and transport processes: A special survey I and II. *J. Non Equilib. Thermodyn.* **21**, 1–16 (1996)
19. Maugin, G.A.: *The Thermomechanics of Nonlinear Irreversible Behaviors: An introduction*. World Scientific, Singapore (1999)
20. Maugin, G.A., Muschik, W.: Thermodynamics with internal variables. Part I. General concepts. *J. Non Equilib. Thermodyn.* **19**, 217–249 (1994)

21. Maugin, G.A., Muschik, W.: Thermodynamics with internal variables. Part II. Applications. *J. Non Equilib. Thermodyn.* **19**, 250–289 (1994)
22. Verhas, J.: *Thermodynamics and Rheology*. Kluwer, Dordrecht (1997)
23. Weiss, W., Müller, I.: Light scattering and extended thermodynamics. *Cont. Mech. Thermodyn.* **7**, 123–177 (1995)
24. Weiss, W.: Zur Hierarchie der erweiterten Thermodynamik. Dissertation, TU Berlin (1990)
25. Weiss, W.: Continuous shock structure in extended thermodynamics. *Phys. Rev. E Part A* **52**, 5760 (1995)
26. Dreyer, W., Struchtrup, H.: Heat pulse experiments revisited. *Cont. Mech. Thermodyn.* **5**, 3–50 (1993)
27. Struchtrup, H.: Der zweite Schall in der Literatur der Festkörperphysik eine kritische Durchsicht. Diploma thesis, TU Berlin (1991)
28. Liu, I.S., Müller, I., Ruggeri, T.: Relativistic thermodynamics of gases. *Annal. Phys.* **169**, 191–219 (1986)
29. Kremer, G.M., Müller, I.: Thermal Conductivity and dynamic pressure in extended Thermodynamics of chemically reacting mixtures of gases. *Ann. de l'Inst. H. Poincaré, Sect. A, Tome* **69**(3), 309–334 (1998)
30. Struchtrup, H.: An extended moment method in radiative transfer. The matrices of mean absorption and scattering coefficients. *Annal. Phys.* **257**, 111–135 (1997)
31. Struchtrup, H.: Zur irreversiblen Thermodynamik der Strahlung. Dissertation, TU Berlin (1996)
32. Reitebuch, D., Weiss, W.: Application of high moment theory to the plane couette flow. *Cont. Mech. Thermodyn.* **11**, 217–225 (1999)
33. Barbera, E.: Onset of Rayleigh-Bénard convection in gases—classical and extended thermodynamics. *Cont. Mech. Thermodyn.* **16**, 337–346 (2004)
34. Donato, A., Ruggeri, T.: Similarity solutions and strong shocks in extended thermodynamics of rarefied gas. *J. Math. Anal. Appl.* **251**, 395–405 (2000)
35. Müller, I., Ruggeri, T.: Stationary Heat Conduction in Radially Symmetric Situations - An Application of Extended Thermodynamics. *J. Non Newtonian Fluid Mech.* **119**, 139–143 (2004)
36. Barbera, E., Müller, I.: Inherent Frame Dependence of Thermodynamic Fields in a Gas. *Act. Mech.* **184**, 205–216 (2006)
37. Barbera, E., Müller, I.: Secondary heat flow between confocal ellipses - an application of extended thermodynamics. *J. Non Newtonian Fluid Mech.* **153**, 149–156 (2008)
38. Bhatnagar, P.L., Gross, E.P., Krook, M.: A model for collision processes in gases. I. Small amplitude processes in charged and neutral one-component systems. *Phys.Rev.* **94**, 511–525 (1954)
39. Truesdell, C.: The physical components of vector and tensor. *ZAMM* **33**, 345–356 (1953)
40. Müller, I.: *Thermodynamics*. Pitman, London (1996)
41. Wendt, G.: Statische Felder und stationäre Strome. In: Flügge, S. (ed.) *Handbuch der Physik XVI*, pp. 1–164. Springer-Verlag, Heidelberg (1958)
42. Barbera, E., Müller, I., Sugiyama, M.: On the temperature of a rarefied gas in non-equilibrium. *Meccanica* **34**, 103–113 (1999)
43. Müller, I., Strehlow, P.: Kinetic temperature and thermodynamic temperature. In: Ripple, C. *Temperature: Its Measurement and Control in Science and Industry*, Vol. 7, American Institute of Physics, Reinhold (2003)
44. Casas-Vázquez, J., Jou, D.: Temperature in non-equilibrium states: A review of open problems and current proposals. *Rep. Prog. Phys.* **66**, 1937–2023 (2003)
45. Serdyukov, S.I.: On the definitions of entropy and temperature in the extended thermodynamics of irreversible processes. *C.R. Physique* **8**, 93–100 (2007)
46. Casas-Vázquez, J., Jou, D.: Extended Irreversible thermodynamics and non-equilibrium temperature. *Atti Acc. Perol. Peric. LXXXVI* (Suppl. I) (2008) pp. 1–12